

1 Constraining the Sea Quark Distributions Through 2 W Cross-Section Ratios Measured in pp Collisions at 3 STAR

4 **M. Posik for the STAR Collaboration**

5 Temple University, Philadelphia, PA USA

6 E-mail: posik@temple.edu

7 **Abstract.** Although the precision to which we know the unpolarized parton distribution
8 functions (PDFs) of the nucleon has improved over the years, there remain kinematic regions
9 where more data are needed to constrain PDFs, such as the ratio of the sea quark distributions
10 \bar{d}/\bar{u} near the valence region. Furthermore, different measurements appear to suggest different
11 high- x behaviors of this ratio. The W cross-section ratio (W^+/W^-) in pp collisions is sensitive
12 to the unpolarized sea quark distributions at large Q^2 , set by the W mass, and can be used
13 to help constrain the \bar{d}/\bar{u} ratio. The STAR experiment at RHIC is well equipped to measure
14 the leptonic decays of W bosons produced in pp collisions at center of mass energies of 500 and
15 510 GeV. These proceedings present recent W cross-section ratio results measured by STAR,
16 including preliminary results from data collected in 2017, which double the statistics when
17 combined with the published results based on data samples recorded in 2011-2013.

18 1. Introduction

19 Flavor asymmetry in the proton sea has been measured by several experiments over the years,
20 most notably the NuSea (E866) [1] and SeaQuest (E906) [2] experiments. Both experiments have
21 measured the x dependence of the \bar{d}/\bar{u} distribution in the proton, where x is the fraction of the
22 proton's momentum carried by the struck quark. The measurements from the two experiments
23 agree at low x ($x < \sim 0.25$), but when approaching the valence region ($x > \sim 0.3$) the two
24 measurements seem to suggest different trends. Additional measurements which are sensitive to
25 the \bar{d}/\bar{u} ratio can be included in global analyses, which fit the available world data in order to
26 extract the parton distribution functions (PDFs), to help further constrain the \bar{d}/\bar{u} ratio and
27 provide insights into the large- x behavior.

28 While E866 and SeaQuest measure the \bar{d}/\bar{u} ratio through the Drell-Yan process, W production
29 in pp collisions is also sensitive to the sea quarks. The $W^+(W^-)$ boson is sensitive to the \bar{d} (\bar{u})
30 quark, which is illustrated in equation (1).

$$31 \quad u + \bar{d} \rightarrow W^+ \rightarrow e^+ + \nu, \quad d + \bar{u} \rightarrow W^- \rightarrow e^- + \bar{\nu}. \quad (1)$$

32 At leading order the W cross-section ratio, $\sigma_{W^+}/\sigma_{W^-}$, is proportional to the sea quark PDFs
33 as shown in equation (2) and probes the sea quark distribution at a large $Q^2 \sim M_W^2$, which is
set by the W boson mass [3].

$$\frac{\sigma_{W^+}}{\sigma_{W^-}} \sim \frac{\bar{d}(x_2)u(x_1) + \bar{d}(x_1)u(x_2)}{\bar{u}(x_2)d(x_1) + \bar{u}(x_1)d(x_2)}. \quad (2)$$

2. Experiment and Results

The STAR experiment at RHIC [4] is well suited to measure the W cross-section ratio, as well as W and Z cross sections [5, 6]. The W cross-section ratios were measured in pp collisions at center of mass energy $\sqrt{s} = 500/510$ GeV recorded during the 2009 [5], 2011-2013 [6], and 2017 running periods. The kinematic reach of STAR allows for complimentary measurements at lower \sqrt{s} and larger x compared to those performed at the LHC. Furthermore, the W cross-section ratio measurements also compliment the E866 and SeaQuest measurements, by accessing \bar{d}/\bar{u} at larger Q^2 . In the pseudorapidity region $-1 < \eta < 2$, STAR probes the x range of approximately 0.06 to 0.4, with the majority of the data falling around $x = 0.16$.

There are several subdetectors used to select electrons/positrons from decays of W bosons, as well as separate their charges: the time projection chamber (TPC) [7], used for particle tracking, the barrel electromagnetic calorimeter (BEMC) [8] and endcap electromagnetic calorimeter (EEMC) [9], which are used to measure particle energy and for triggering. The integrated luminosity of each data set is as follows: 345 pb⁻¹ (2011-2013), ~ 350 pb⁻¹ (2017), and the recently completed 2022 data set recorded an additional 450 pb⁻¹.

The W cross-section ratio can be measured experimentally as

$$\frac{W^+}{W^-} = \frac{N_O^+ - N_B^+}{N_O^- - N_B^-} \cdot \frac{\epsilon^-}{\epsilon^+}, \quad (3)$$

where N_O is the number of recorded W boson candidates, N_B is the number of background events estimated from data and Monte Carlo, ϵ is the detection efficiency, and $+/-$ refers to the respective boson candidate's charge.

Electrons and positrons from leptonic decays of W candidates are selected using methodologies previously developed by STAR [5, 6, 10].

The W^+ and W^- background contributions measured in the BEMC for the 2017 data set are shown in Figs. 1 and 2, respectively. The background contributions include events from $W \rightarrow \tau + \nu$, $Z \rightarrow ee$, QCD, and those related to the fact that STAR is equipped with only one endcap calorimeter (“second EEMC” background). The QCD and second EEMC backgrounds are estimated using data, while the other background contributions are computed from Monte Carlo. An estimate of the amount of QCD background is determined from the transverse energy, E_T , distribution that fails the criteria requiring an overall momentum imbalance due to the neutrino in a $W \rightarrow e\nu$ decay escaping detection. This distribution is dominated by QCD type events. The second EEMC background is an estimate of the background caused by an escaping jet's p_T being misidentified as the neutrino's missing p_T . Also included in the figures are the Monte Carlo simulation of the W decay signal (based on Pythia 6.4.22 [11] and GEANT [12]), and combination of the Monte Carlo signal and background contributions, which describes the measured E_T distribution fairly well. When the final analysis cut requiring $E_T > 25$ GeV is applied, there is little background contamination remaining relative to the W signal.

Figure 3 shows the preliminary W cross-section ratio from the 2017 data set plotted as a function of the lepton pseudorapidity and compared to the results from the STAR 2011-2013 [6] data sets. The vertical bars represent the statistical uncertainties, while the boxes represent systematic uncertainties. The bands and curves correspond to theoretical calculations based on different PDF sets [13, 14, 15, 16, 17, 18] and frameworks [19, 20]. Beginning from the STAR 2011-2013 results, Fig. 4 shows how the statistical precision improves when adding the statistics from the 2017 data set and finally the projected precision by adding the 2022 data set.

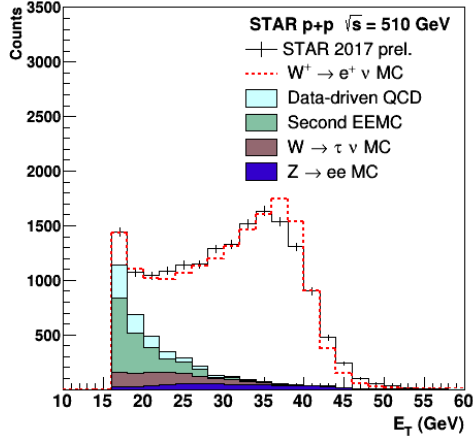


Figure 1. E_T distributions for W^+ (positrons) candidates and estimated background contributions.

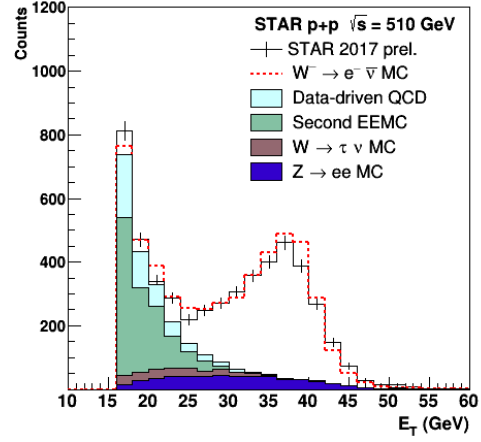


Figure 2. E_T distributions for W^- (electrons) candidates and estimated background contributions.

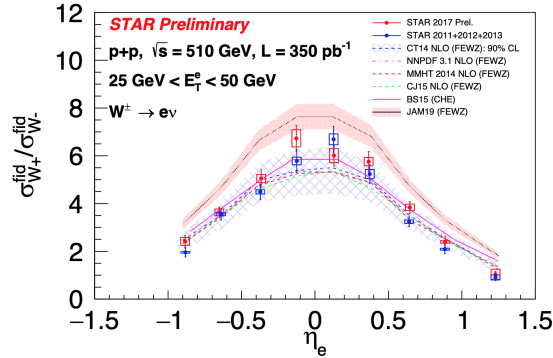


Figure 3. STAR 2017 preliminary W cross-section ratio plotted as a function of lepton pseudorapidity and compared to STAR 2011-2013 results [6] and various PDF sets [13, 14, 15, 16, 17, 18].

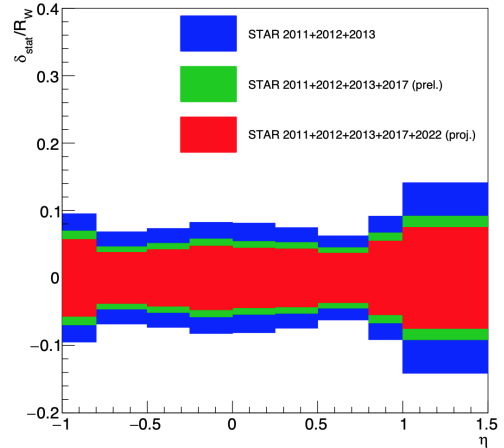


Figure 4. Improvement in statistical precision of the W cross-section ratio when adding the statistics from the 2017 and 2022 data sets.

76 Several studies [6, 21, 22] assessing the impact that the STAR 2011-2013 W cross-section
 77 ratio data has on the sea quark distributions found a modest improvement on the uncertainty
 78 associated with the \bar{d}/\bar{u} PDF, as well as other light quark PDFs [6, 22]. While these data do
 79 not carry as much weight as the more direct NuSea and SeaQuest measurements in constraining
 80 the \bar{d}/\bar{u} distribution, STAR is able to provide new and complimentary data which does provide
 81 some additional constraint on the distribution.

82 3. Summary

83 STAR has measured the W cross-section ratio in pp collisions at $\sqrt{s} = 500$ GeV and 510
84 GeV. These measurements provide large Q^2 data that are sensitive to the \bar{d}/\bar{u} ratio in the
85 kinematic range of about $0.06 < x < 0.4$, which will help constrain the sea quark PDFs and
86 complement the E866 and SeaQuest measurements. Furthermore, the lower \sqrt{s} results from
87 STAR are complementary to the LHC W production measurements by probing larger x . The
88 STAR preliminary W cross-section ratio results from the 2017 data set totaling 350 pb^{-1} have
89 been presented. The statistical precision of the W cross-section ratio will be further improved
90 once the 2022 data set is analyzed, which recorded an additional 450 pb^{-1} .

91 4. Acknowledgments

92 We thank the RHIC Operations Group and RCF at BNL. This work is supported by U.S. DOE
93 Office of Science and DOE-310385.

94 5. References

- 95 [1] R. S. Towell *et al.*, Phys. Rev. D, **64**, 052002 (2001).
96 [2] J. Dove *et al.*, Nature 590 (7847), 561 (2021).
97 [3] C. Bourrely and J. Soffer, Nucl. Phys. B **423**, 329 (1994).
98 J. Soffer, C. Bourrely, and F. Buccella, arXiv:1402.0514 (2014).
99 [4] K. H. Ackermann *et al.* (STAR), Nucl. Instrum. Meth. A **499**, 624 (2003).
100 [5] L. Adamczyk *et al.* (STAR), Phys. Rev. D **85**, 092010 (2012).
101 [6] J. Adam *et al.* (STAR), Phys. Rev. D **103**, 012001 (2021).
102 [7] M. Anderson *et al.* (STAR), Nucl. Instrum. Meth. A **499**, 659 (2003).
103 [8] M. Beddo *et al.* (STAR), Nucl. Instrum. Meth. A **499**, 725 (2003).
104 [9] C. Allgower *et al.* (STAR), Nucl. Instrum. Meth. A **499**, 740 (2003).
105 [10] J. Adam *et al.* (STAR), Phys. Rev. D **99**, 051102 (2019).
106 [11] T. Sjostrand, S. Mrenna, and P. Skands, *Pythia 6*, <https://pythia6.hepforge.org>.
107 [12] S. Agostinelli *et al.*, Nucl. Instrum. Meth. A **506**, 250 (2003).
108 [13] J. Gao *et al.*, Phys. Rev. D, **89**, 3, 033009 (2014).
109 [14] L. A. Harland-Lang, *et al.*, EPJ C, **75**, 5, 204 (2015).
110 [15] R. D. Ball *et al.*, Eur. Phys. J. C **77**, 663 (2017).
111 [16] C. Bourrely and J. Soffer, Nucl. Phys. A, **941**, 307 (2015).
112 [17] A. Accardi, L. T. Brady, W. Melnitchouk, J. F. Owens, and N. Sato, Phys. Rev. D **93**, 114017 (2016).
113 [18] N. Sato, C. Andres, J. J. Ethier, and W. Melnitchouk (JAM), Phys. Rev. D **101**, 074020 (2020).
114 [19] Y. Li and F. Petriello, Phys. Rev. D **86**, 094034 (2012).
115 [20] D. de Florian and W. Vogelsang, Phys. Rev. D **81**, 094020 (2010).
116 [21] C. Cocuzza, W. Melnitchouk, A. Metz, and N. Sato (Jefferson Lab Angular Momentum (JAM) Collaboration)
117 Phys. Rev. D **104**, 074031 (2021).
118 [22] Sanghwa Park, Alberto Accardi, Xiaoxian Jing, J. F. Owens (CJ), arXiv:2108.05786, DIS Proceedings (2021),
119 <https://arxiv.org/abs/2108.05786>.